Image analysis via the general theory of moments*

Michael Reed Teague†

Air Force Weapons Laboratory, Beam Control Systems Branch, Kirtland AFB, Albuquerque, New Mexico 87117

(Received 1 November 1979)

Two-dimensional image moments with respect to Zernike polynomials are defined, and it is shown how to construct an arbitrarily large number of independent, algebraic combinations of Zernike moments that are invariant to image translation, orientation, and size. This approach is contrasted with the usual method of moments. The general problem of two-dimensional pattern recognition and three-dimensional object recognition is discussed within this framework. A unique reconstruction of an image in either real space or Fourier space is given in terms of a finite number of moments. Examples of applications of the method are given. A coding scheme for image storage and retrieval is discussed.

INTRODUCTION

The general problem to be considered is that of characterizing, evaluating, and manipulating visual information that is present in the image plane or any other plane (e.g., the Fourier plane) of an optical system. An example of such usage could be the automatic identification of a pattern, size, and orientation measurements of an image, or the automatic extraction of the coordinates of an algorithm search point that is known to be located somewhere in the image. In all such cases the general method of moments furnishes a solution of the problem. Moreover, at present with dedicated digital processors these operations may be performed in real time, for example, at TV frame rates. In addition, it appears that these methods have potential for coping with the difficult problem of real time sensing of the time varying aberrations in an optical system degraded by, for example, atmospheric turbulence or thermal blooming.[1–4] (This last problem, however, will not be discussed further in the present paper.) While moment methods are generally employed with video-digital processors, we will briefly indicate how moments could be extracted in a coherent optical processor that might be utilized in a high-speed film scanner that automatically identifies biological patterns.

Historically, Hu[5] published the first significant paper on the use of image moment invariants for two-dimensional pattern recognition applications; his approach is based on the work of the nineteenth century mathematicians Boole, Cayley, and Sylvester, on the theory of algebraic forms. More recently, Dudani *et al.*[6] used moment invariants in automatic aircraft identification algorithms. The well-known properties of second- and lower-order moments are summarized in Sec. I, while Sec. II treats the question of what is gained by including higher-order moments in the analysis of an image. In Sec. III, rotation and reflection invariance is studied using Zernike moments. This approach is unusually simple and in a straightforward manner allows moment invariants to be constructed to an arbitrarily high order and in addition furnishes an elementary procedure to determine whether a given set of moment invariants is composed of functionally independent members.

If Zernike moments are related to the usual moments, the invariants constructed in this paper are largely equivalent to those of Hu; however, as may be seen in Appendices A and B, if it is necessary to use higher-order moment invariants, the expressions based directly on Zernike moments are enormously simpler than those based on the usual central moments. In the statistical image recognition problem, the weights assigned to the various moment invariants used as pattern identifiers are crucially important. It is interesting that the weights that occur naturally in the present paper differ from those in Ref. 5. In addition, the present paper treats the general problem of object size or range normalization of the moments.

At the outset it should be stressed that the use of low-order moments, for example, centroid position and moments of inertia, is commonplace in many disciplines. On the other hand, it is well known[7] that by using a sufficiently large number of image moments we in principle recapture all the image information, but then we would merely have replaced one total description (approximately infinite number of pixel intensities) by an equivalent one (approximately infinite number of moments). The interesting question is how well the method of moments works for a particular application if one considers moments up through, e.g., fifth or tenth order. For example, a single video image may contain 10^4–10^8 bits of information, while a photographic image can contain orders of magnitude more. Often, however, the quantitative information that is needed from an image is more likely to be of the order of 10 or 20 real numbers. Then the method of moments furnishes a general systematic procedure for extracting a set of quantitative features from an image.

I. PROPERTIES OF LOW-ORDER MOMENTS

In all cases we consider a finite image plane and all integrals not otherwise designated are over this finite image plane. We start by recalling certain well-known[8,9] properties of the lowest-order moments. Denoting the image plane irradiance distribution by $f(x,y)$ we have the zero-order moment

$$\mu_{00} = \iint dx\,dy f(x,y) \tag{1}$$

representing the total image power. The first-order moments

$$\mu_{10} = \iint dx\,dy\,x f(x,y), \tag{2}$$

$$\mu_{01} = \iint dx\,dy\,y f(x,y) \tag{3}$$

 0030-3941/80/080920-11$00.50

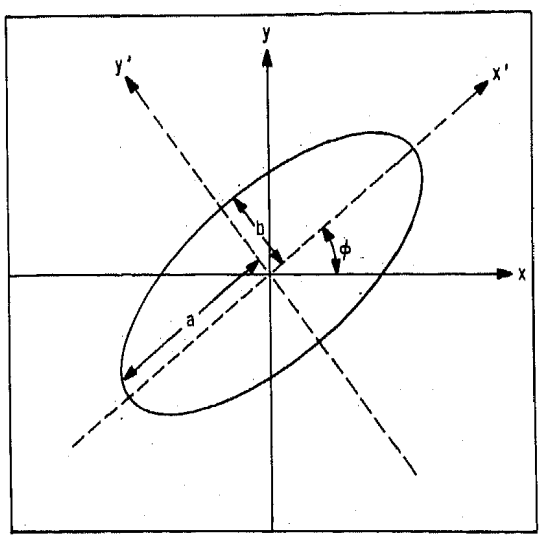

FIG. 1. Image ellipse.

locate the centroid of the irradiance distribution, i.e., $\bar{x} = \mu_{10}/\mu_{00}$, $\bar{y} = \mu_{01}/\mu_{00}$, and the second-order moments

$$\mu_{20} = \iint dx\,dy f(x,y)x^2, \tag{4}$$

$$\mu_{11} = \iint dx\,dy f(x,y)xy, \tag{5}$$

$$\mu_{02} = \iint dx\,dy f(x,y)y^2 \tag{6}$$

characterize the size and orientation of the image. In fact, if only moments up through second order are considered, the original image is completely equivalent to a constant irradiance ellipse having definite size, orientation, and eccentricity and centered at the image centroid. In this section we assume the coordinate origin has been chosen to coincide with the image centroid.

The parameters of this "image ellipse" are (referring to Fig. 1)

$$a = \left(\frac{\mu_{20} + \mu_{02} + [(\mu_{20} - \mu_{02})^2 + 4\mu_{11}^2]^{1/2}}{\mu_{00}/2}\right)^{1/2}, \tag{7}$$

$$b = \left(\frac{\mu_{20} + \mu_{02} - [(\mu_{20} - \mu_{02})^2 + 4\mu_{11}^2]^{1/2}}{\mu_{00}/2}\right)^{1/2} \tag{8}$$

for the semimajor and semiminor axes, respectively, and

$$\phi = (1/2)\tan^{-1}\left(\frac{2\mu_{11}}{\mu_{20} - \mu_{02}}\right) \tag{9}$$

for the ellipse tilt angle. The irradiance of the image ellipse is

$$F = \mu_{00}/\pi ab \tag{10}$$

inside the ellipse and zero outside.

These results follow[9] from a consideration of the rotation transformation properties of the second-order moments:

$$\begin{bmatrix}\mu_{20}\\ \mu_{11}\\ \mu_{02}\end{bmatrix} = \begin{bmatrix}\frac{1+\cos 2\phi}{2} & -\sin 2\phi & \frac{1-\cos 2\phi}{2}\\ \frac{\sin 2\phi}{2} & \cos 2\phi & -\frac{\sin 2\phi}{2}\\ \frac{1-\cos 2\phi}{2} & \sin 2\phi & \frac{1+\cos 2\phi}{2}\end{bmatrix}\begin{bmatrix}\mu'_{20}\\ \mu'_{11}\\ \mu'_{02}\end{bmatrix}, \tag{11}$$

where ϕ is the rotation angle. The fact that 2ϕ appears is a consequence of the ellipse being unchanged by a 180° rotation.

There is an ambiguity in the tilt angle ϕ of the ellipse which we resolve by choosing ϕ always to be the angle between the x axis and the semimajor axis, i.e., by definition

$$a \geq b.$$

Secondly, we pick the principal value of the function arc tangent such that

$$-\pi/2 \leq \tan^{-1}x \leq \pi/2.$$

With these conventions we arrive at the results for the tilt angle that are given in Table I.

Finally, we point out that one may show[9] by an application of the classical Schwarz's inequality that the image ellipse exists with real a and b if and only if the function $f(x,y)$ is non-negative, which is true for irradiance distributions, but not for amplitude distributions.

II. INVERSE MOMENT PROBLEM: OPTIMAL RECONSTRUCTION OF AN IMAGE

We now look at higher-order moments which in the general case are defined by

$$M_{jk} = \iint dx\,dy f(x,y)x^j y^k. \tag{12}$$

To investigate the information content of the higher-order moments, we begin by considering the inverse problem: Given only some (finite) set of moments of an image, how well can we reconstruct the image? We will give two equivalent answers to this question. The first is a direct approach and the second, which is computationally simpler, uses orthogonal moments based on Legendre polynomials. Both methods furnish our definition of the best reconstruction of an image based on a finite set of its moments, i.e., they produce a continuous irradiance function whose moments match the given

TABLE I. Ellipse Tilt Angle for Various Cases of the signs of the second moments.

$\mu_{20} - \mu_{02}$	μ_{11}	ϕ	
Zero	Zero	0	$\xi \equiv \frac{2\mu_{11}}{\mu_{20} - \mu_{02}}$
Zero	Positive	+45°	
Zero	Negative	−45°	
Positive	Zero	0	
Negative	Zero	−90°	
Positive	Positive	$(1/2)\tan^{-1}\xi$	$(0 < \phi < 45°)$
Positive	Negative	$(1/2)\tan^{-1}\xi$	$(-45° < \phi < 0)$
Negative	Positive	$(1/2)\tan^{-1}\xi + 90°$	$(45° < \phi < 90°)$
Negative	Negative	$(1/2)\tan^{-1}\xi - 90°$	$(-90° < \phi < -45°)$

set. The methods and outlook of this section lead naturally to the approach of Sec. III where symmetry properties of moments are treated.

It should be mentioned that the inverse moment problem we are considering in this section is a special case of a much more general, extensively studied, mathematical problem formally stated by Stieljes[10] in the last century.

As we stated before, one of our primary interests is in determining how well an image may be characterized by a small finite set of its moments. Moreover, the infinite set of all moments contains exactly the same information as the original image, the connection between the two descriptions being made via the characteristic function. However, we will point out that the characteristic function is not useful for treating a small set of moments.

Finally, we point out that since we only consider image planes of finite extent, we always choose the unit of length such that the maximum distance of any point in the image plane from the center of the image plane is less than unity, e.g., we can take the image plane over which we calculate moments to be the region

$$\begin{aligned} x &\in (-1,+1), \\ y &\in (-1,+1). \end{aligned} \tag{13}$$

(For a rectangular format image plane, we would just require that one of the maximum distances be less than unity, e.g., 0.8.) With this choice, higher-order moments will, in general, have increasingly smaller numerical values. Later we will see that the moments are related to the coefficients in an expansion that reconstructs $f(x,y)$, and we improve the convergence properties by arranging to have $|x|$ and $|y|$ less than unity.

A. Characteristic function

Consider now the characteristic function[11] for the irradiance function $f(x,y)$:

$$F(\xi,\eta) = \iint dx\,dy\, e^{-i2\pi(\xi x+\eta y)} f(x,y). \tag{14}$$

Since in cases of interest to us $f(x,y)$ is at worst piecewise continuous, and the integration limits are finite, $F(\xi,\eta)$ is a continuous function and may be expanded as a power series in ξ,η. To see what the expansion is, note that

$$\begin{aligned} F(\xi,\eta) &= \iint dx\,dy \sum_{j=0}^{\infty} \frac{(-i2\pi\xi x)^j}{j!} \sum_{k=0}^{\infty} \frac{(-i2\pi\eta y)^k}{k!} f(x,y) \\ &= \sum_{j=0}^{\infty} \sum_{k=0}^{\infty} \frac{(-i2\pi)^{j+k}}{j!k!} M_{jk} \xi^j \eta^k, \end{aligned} \tag{15}$$

where the interchange of order of summation and integration is permissible for the reason given in the last sentence. Thus we see that the moment M_{jk} is essentially the expansion coefficient of the $\xi^j\eta^k$ term in a power series expansion of the characteristic function of the image irradiance function $f(x,y)$. Given $F(\xi,\eta)$, $f(x,y)$ is given by the inversion formula

$$\begin{aligned} f(x,y) &= \int_{-\infty}^{\infty} d\xi \int_{-\infty}^{\infty} d\eta\, e^{i2\pi(\xi x+\eta y)} F(\xi,\eta) \\ &= \int_{-\infty}^{\infty} d\xi \int_{-\infty}^{\infty} d\eta\, e^{i2\pi(\xi x+\eta y)} \\ &\quad \times \sum_{j=0}^{\infty} \sum_{k=0}^{\infty} \frac{(-i2\pi)^{j+k}}{j!k!} M_{jk} \xi^j \eta^k. \end{aligned} \tag{16}$$

Now, however, the order of summation and integration in Eq. (48) cannot be interchanged, or one will immediately derive the false conclusion that the original intensity function $f(x,y)$ is an infinite series—all of whose terms are derivatives of delta functions located at the origin. The conclusion is that the power series expansion for $F(\xi,\eta)$ cannot be integrated term by term. It must first be summed in closed form to obtain a function that vanishes sufficiently fast as $\sqrt{\xi^2+\eta^2} \to \infty$, and then integrated. In particular, if one knows only a finite small set of moments, one cannot use a truncated series in Eq. (47) and learn about the original function $f(x,y)$. The same conclusion follows if the moment generating function (which has the same relation to the characteristic function as the Laplace transform has to the Fourier transform) is used.

B. Moment matching approach

In Sec. III we will see that one must, on the basis of rotational invariance, consider all moment M_{jk} of a given order $N = j + k$ together on the same footing. Suppose now that one knows all moments M_{jk} up to a given order $N_{\max}$. We now show that no matter what type of function $f(x,y)$ gave rise to the given finite set of moments, it is possible to obtain a *continuous* function $g(x,y)$ whose moments exactly match those of $f(x,y)$ up to the given order $N_{\max}$. We assert that the given function may be expressed in the form

$$\begin{aligned} g(x,y) = g_{00} + g_{10}\,x + g_{01}\,y + g_{20}\,x^2 + g_{11}\,xy + g_{02}\,y^2 \\ + g_{30}x^3 + g_{21}\,x^2y + g_{12}\,xy^2 + g_{03}\,y^3 + \cdots, \end{aligned} \tag{17}$$

where the constant coefficients g_{jk} are now to be determined such that the moments of $g(x,y)$ match those of $f(x,y)$; i.e.,

$$\int_{-1}^{+1} dx \int_{-1}^{+1} dy\, g(x,y) x^j y^k \equiv M_{jk}. \tag{18}$$

As an example, we determine the coefficients such that $g(x,y)$ has moments that match those of $f(x,y)$ up through third order. Applying Eq. (18) to Eq. (17) for the ten cases of $j + k \le 3$, we produce ten algebraic equations, which we write in matrix form:

$$\begin{bmatrix} 1 & \frac{1}{3} & \frac{1}{3} \\ \frac{1}{3} & \frac{1}{5} & \frac{1}{9} \\ \frac{1}{3} & \frac{1}{9} & \frac{1}{5} \end{bmatrix} \begin{bmatrix} g_{00} \\ g_{20} \\ g_{02} \end{bmatrix} = (1/4) \times \begin{bmatrix} M_{00} \\ M_{20} \\ M_{02} \end{bmatrix}, \tag{19}$$

$$\begin{bmatrix} \frac{1}{3} & \frac{1}{5} & \frac{1}{9} \\ \frac{1}{5} & \frac{1}{7} & \frac{1}{15} \\ \frac{1}{9} & \frac{1}{15} & \frac{1}{15} \end{bmatrix} \begin{bmatrix} g_{10} \\ g_{30} \\ g_{12} \end{bmatrix} = (1/4) \times \begin{bmatrix} M_{10} \\ M_{30} \\ M_{12} \end{bmatrix}, \tag{20}$$

$$g_{11} = (9/4) M_{11}. \tag{21}$$

[The three remaining equations are obtained by interchanging $j \rightleftharpoons k$ in Eq. (20). Note in particular we did not get a 10×10 coupled set of equations, but instead a number of smaller dimensional coupled sets. We immediately display the answer for $g(x,y)$!]

$$
\begin{aligned}
16g(x,y) &= (14M_{00} - 15M_{20} - 15M_{02}) \\
&+ (90M_{10} - 105M_{30} - 45M_{12})x \\
&+ (90M_{01} - 105M_{03} - 45M_{21})y \\
&+ (-15M_{00} + 45M_{20})x^2 + 36M_{11}xy \\
&+ (-15M_{00} + 45M_{02})y^2 + (-105M_{10} + 175M_{30})x^3 \\
&+ (-45M_{01} + 135M_{21})x^2y + (-45M_{10} + 135M_{12})xy^2 \\
&+ (-105M_{01} + 175M_{03})y^3. \qquad (22)
\end{aligned}
$$

If we wanted $g(x,y)$ to match the moments of $f(x,y)$ only through second order, Eq. (22) would still be correct if all the third-order moments were set to zero on the right-hand side and, in addition, all terms of degree three were dropped. Conversely, if, for example, fourth- and fifth-order moments were being matched also, then the coefficients already given in Eq. (22) would change and also there would be additional terms of degree four and five.

In the general case, one immediately infers that by solving a *linear* coupled set of equations one can always exhibit a continuous function that produces moments matching a finite set of given moments. In Sec. II C, it will be obvious that the method recreates *exactly* the original function $f(x,y)$ as increasingly more moments are matched, within the limitations of the well-known Gibbs phenomena[12] at jump discontinuities of the original intensity pattern. The disadvantages of this direct approach are (i) the coefficients already determined change as more moments are included, and (ii) one must solve increasingly large coupled sets of equations.

C. Method of orthogonal moments

In the language of orthogonal functions, we notice that the definition of the general moment

$$M_{jk} = \iint dx\,dy f(x,y)x^j y^k$$

has the form of the projection of the irradiance function $f(x,y)$ onto the monomial x^jy^k. Unfortunately, the basis set $\{x^jy^k\}$, while complete (Weierstrass approximation theorem), is not orthogonal. We now show that by introducing the notion of orthogonal moments it is possible to make a "best" reconstruction of $f(x,y)$ in the sense of Sec. B, given only a finite set of its moments. Such an approach is suggested by remarks in Ref. 13.

We need a set of basis functions, orthogonal over a finite interval and in the present case it is natural to choose the weighting function to be unity. This uniquely specifies the Legendre polynomials as the appropriate set. At this point we stress that we consider x and y to be dimensionless variables, giving the location of a given pixel in the image space, and not dimensional distances. Thus we may freely add x and x^2, for example. Then, since $f(x,y)$ is assumed (piecewise) continuous over the basic interval, we can write

$$f(x,y) = \sum_{m=0}^{\infty}\sum_{n=0}^{\infty} \lambda_{mn}P_m(x)P_n(y), \qquad (23)$$

where $P_m(x)$ is the usual Legendre polynomial[14] with normalization

$$\int_{-1}^{+1} dx\,P_m(x)P_{m'}(x) = \frac{2}{2m+1}\delta_{mm'}. \qquad (24)$$

The *orthogonal* (Legendre) moment of $f(x,y)$ is defined by

$$\lambda_{mm} \equiv \frac{(2m+1)(2n+1)}{4}\iint dx\,dy f(x,y)P_m(x)P_n(y). \qquad (25)$$

We now show that the set $\{\lambda_{mn}\}$ is simply related to the usual moments $\{M_{mn}\}$. The Legendre polynomial may be written

$$P_m(x) = \sum_{j=0}^{m} C_{mj}x^j, \qquad (26)$$

where the coefficients C_{mj} are given in Ref. 14.

Then, inserting Eq. (26) into Eq. (25), we get the desired connection

$$\lambda_{mn} = \frac{(2m+1)(2n+1)}{4}\sum_{j=0}^{m}\sum_{k=0}^{n} C_{mj}C_{nk}M_{jk}. \qquad (27)$$

Thus, for example, $\lambda_{00} = M_{00}/4$, $\lambda_{10} = (3/4)M_{10}$, $\lambda_{01} = (3/4)M_{01}$, $\lambda_{20} = (5/4)[3/2\,M_{20} - (1/2)M_{00}]$, $\lambda_{11} = (9/4)M_{11}$, $\lambda_{02} = (5/4)[(3/2)M_{02} - (1/2)M_{00}]$, etc. It is straightforward to show that the usual moments depend at most on the Legendre moments of the same order and lower, and conversely.

Now the infinite series expansion in Eq. (23) is basically a summation by infinite rows and in fact is never used. Instead, one sums along finite diagonals and, truncating at a given finite order $N_{\max}$, we have

$$f(x,y) \cong \sum_{N=0}^{N_{\max}}\sum_{n=0}^{N} \lambda_{N-n,n}P_{N-n}(x)P_n(y). \qquad (28)$$

This is the basic equation of the method of Legendre moments. The coefficients λ_{mn}, $(m = N - n)$, are final; if $N_{\max}$ is increased, the previously determined λ_{mn} do not change. In addition, not only do the Legendre moments λ_{mn} of the right-hand side of Eq. (28) match those of the original image distribution $f(x,y)$ up to a given order $N_{\max}$, but so do the usual moments M_{jk} match to the same order. In fact, to a given order, the right-hand side of Eq. (28) and the function $g(x,y)$ of Sec. II B are identical; the terms have just been regrouped. The big advantage of the present approach is that to get the Legendre moments, we need not solve any coupled algebraic equations. We just calculate them from Eq. (27) using known Legendre polynomial coefficients.

A possibly unexpected feature is that, in general, the moment matching function, such as $g(x,y)$ above, is not necessarily positive definite, even if the original function $f(x,y)$ was. If the lack of positive definiteness of the approximating function $g(x,y)$ is objectionable in certain applications, there is a way to get around this feature. Since $f(x,y) \geq 0$, one can work first with $\sqrt{f(x,y)}$, which is real, and find $g(x,y)$, which matches the moments of $\sqrt{f(x,y)}$. Then, one uses $g^2(x,y)$ as a positive definite approximation to $f(x,y)$.

In Figs. 2 and 3 we show examples of the reconstruction of an image from its moments. In both cases the input $f(x,y)$ is a binary-valued figure which for illustration purposes we have taken simply as capitalized letters. For convenience we took the image plane to be a 21×21 pixel array (then the step size is 0.1). Following the input irradiance in each figure, we show the reconstructed images obtained by including increasingly higher-order moments. Actually, the reconstruction function $g(x,y)$ is continuous across the image plane and what we have shown in these figures is a thresholded version of $g(x,y)$ to facilitate viewing the results. As expected, the second-order

FIG. 2. Reconstruction of the letter E. Top row, left to right: original input image, reconstructed image with up through 2nd-order moments, up through 3rd order, up through 4th order. Succeeding rows in left to right order show effect of adding up through 5th-order through up through 16th-order moments.

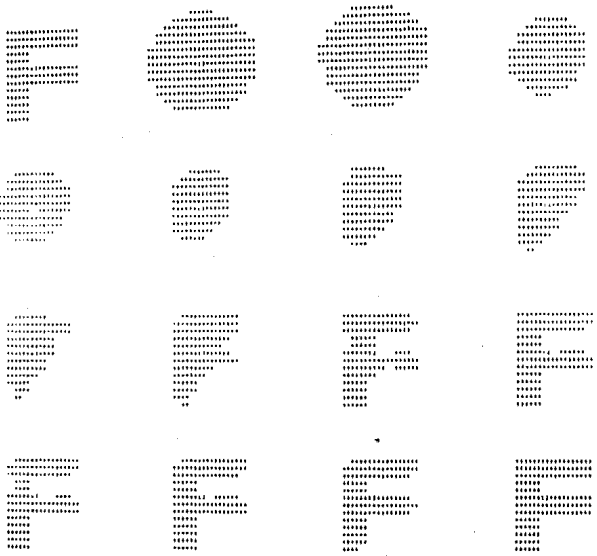

FIG. 3. Reconstruction of letter F. Description of Fig. 2 applies except the effect of adding up through 2nd order through up through 15th order is shown and last entry includes all moments through 18th order. The image for 16th and 17th order were very similar to that for the 15th order.

reconstruction is simply a quantized version of an ellipse. In Fig. 2 the reason odd moments are nonvanishing is that the input figure was intentionally not centered horizontally. It is perhaps surprising that in both cases, the inclusion of third-, fourth-, and fifth-order moments has little effect on the "quality" of the reconstruction, and one begins to see the input shapes emerging only with the inclusion of higher-order moments. In Table II we have shown the average pixel error in the reconstruction function, i.e., the average pixel error between the continuous $g(x,y)$ (not the thresholded version) and the input function $f(x,y)$. In both cases (Figs. 2 and 3) the thresholded version of the reconstruction does not change appearance if increasingly more moments are included; however, the average pixel error steadily decreases as more moments are added. The fact that the average pixel error remains relatively large is simply a reflection of the fact that we are fitting a 441-pixel image with a much smaller number of moments.

The point of this section and the examples just discussed is to show explicitly that moments may describe an image or any other set of two-dimensional data as well as is needed for a given application. In particular, while second-order moments contain only the simplest estimates of size, shape, and orientation of the image data, a larger (but still relatively small) finite set of moments may characterize an image extremely well.

In addition, we will see in Sec. III that moments have symmetry properties that allow a very economical numerical encoding of the image, or alternatively furnish a basis for automatic pattern recognition schemes.

III. SYMMETRY INVARIANTS AND ZERNIKE MOMENTS

When a symmetry operation is applied to an image, its irradiance function changes

$$F(x,y) \rightarrow F'(x,y),$$

and correspondingly the moments change

$$M_{jk} \rightarrow M'_{jk}.$$

However, for the simplest operations, namely, size changes, translations, rotations, or reflections, it is possible to "normalize" the set of moments so that they are invariant to these operations.

A. Translation and range invariance of moments

A transverse motion of the object with respect to the system optic axis produces a displacement of the image in the xy plane, while object motion parallel to the optic axis produces a change in image size.

TABLE II. Average relative pixel errors in the reconstructed irradiance functions of Figs. 2 and 3. Errors are in %.

Maximum order of moments included	E	F
2	133	149
3	132	149
4	103	118
5	102	119
6	90	102
7	91	101
8	87	98
9	83	93
10	81	92
11	74	81
12	67	75
13	61	65
14	54	60
15	47	56
16	46	51
17	40	48
18	36	43
19	33	39
20	27	33

In this section we recall how to define image moments that are invariant to these two transformations.

The coordinates of the image centroid are

$$\bar{x} = M_{10}/M_{00}, \qquad \bar{y} = M_{01}/M_{00}. \tag{29}$$

Central moments μ_{pq} are defined with respect to the image centroid, and it is straightforward to show that the connection between central and raw moments is

$$\mu_{jk} = \sum_{r=0}^{j} \sum_{s=0}^{k} \binom{j}{r} \binom{k}{s} (-\bar{x})^{j-r} (-\bar{y})^{k-s} M_{rs}. \tag{30}$$

The μ_{jk} directly contains information on the size and shape of the image pattern without having a lever arm folded into the numbers, and one sees that a given central moment depends only on usual moments of the same order and lower. It is obvious that central moments are invariant to image translation. Also note that

$$\mu_{10} = \mu_{01} = 0 \tag{31}$$

always. Thus to normalize away translation effects, one works simply with central moments. If the object changes range, the image changes size, and we shall assume the imaging system is such that the new irradiance function is

$$f'(x,y) = f(x/\lambda, y/\lambda), \tag{32}$$

where λ is a scale factor

$$\lambda = R/R' \tag{33}$$

equal to the ratio of object ranges. Under this transformation the moments change

$$\mu'_{pq} = \iint dx\, dy f(x/\lambda, y/\lambda) x^p y^q = \lambda^{2+p+q} \mu_{pq}, \tag{34}$$

and it is clear that the normalized moments

$$\mu_{pq}/(\mu_{00})^{(p+q+2)/2} \tag{35}$$

are invariant to size (range) changes. This normalization corresponds to having the total image power μ_{00} always equal to unity. Such a normalization for size change is, of course, not unique. An alternative choice corresponds to making the (unnormalized) radius of gyration $(\mu_{20} + \mu_{02})^{1/2}$ equal to unity. Then, the general moment must be normalized by $\mu_{pq}/(\mu_{20} + \mu_{02})^{(2+p+q)/4}$.

B. Rotation properties of moments

To arrive at a set of moments "normalized" with respect to rotations is more involved. It is straightforward to show that if the image rotates through an angle ϕ, the moments change according to

$$\mu'_{jk} = \sum_{r=0}^{j} \sum_{s=0}^{k} (-1)^{k-s} \binom{j}{r} \binom{k}{s} (\cos\phi)^{j-r+s} \times (\sin\phi)^{k+r-s} (\mu_{j+k-r-s, r+s}), \tag{36}$$

and we see that the set of moments μ_{jk} of given order $N = j + k$ transform into the set μ'_{jk} of the *same* order $N = j' + k'$, as indicated in Eq. (45). This incidentally shows that all moments of a given order must be treated on equal footing.

Equation (36) is the basis of the work of Hu[5] and the applications of Dudani *et al.*[6] Using the nineteenth century methods of algebraic invariants, Hu derived rotation invariant combinations of moments. We now show a much more straightforward approach to this problem.

As is mentioned in Sec. II, the moments μ_{pq} are basically projections of the function $f(x,y)$ onto the nonorthogonal basis set $\{x^p y^q\}$, and the lack of a simple transformation law of the usual moments μ_{pq} is a reflection of the fact that the basis set has no simple rotation properties. This suggests that new moments should be defined with respect to a set of functions with simple rotation properties. This will allow us to construct in a straightforward manner algebraic combinations of moments that are rotationally invariant.

C. Definition of Zernike moments

A set of orthogonal functions with simple rotation properties and with weight function unity are the well-known Zernike polynomials

$$V_{nl}(x,y) = V_{nl}(\rho\sin\theta, \rho\cos\theta) = R_{nl}(\rho)\exp(il\theta). \tag{37}$$

(We use the notation and normalization of Ref. 15.) These functions are complete over the unit circle and satisfy the relation

$$\iint dx\, dy [V_{nl}(x,y)]^* V_{mk}(x,y) = \pi/(n+1)\delta_{mn}\delta_{kl}, \tag{38}$$

where now the integration is over the unit circle $x^2 + y^2 \leqslant 1$. Moreover, we shall always consider only images that vanish outside the unit circle, and it will be clear from context whether the integration region is over the unit circle or the square defined by Eq. (13), or whether in fact it does not matter which region is chosen. Note also that θ is the angle between radius vector ρ and the y axis, while ϕ is the angle between ρ and the x axis.

Subject to the limitations discussed previously for Legendre moments, the image irradiance function may then be approximated by

$$f(x,y) = \sum_n \sum_l A_{nl} V_{nl}(\rho,\theta), \tag{39}$$

where $n = 0, 1, 2, \ldots, \infty$, and l takes on positive and negative integer values subject to the conditions:

$$n - |l| \text{ is even}, \quad |l| < n. \tag{40}$$

The complex Zernike moment is by definition

$$A_{nl} = [(n+1)/\pi] \iint dx\, dy f(x,y)[V_{nl}(\rho,\theta)]^* = (A_{n,-l})^*. \tag{41}$$

(The second equal sign holds because f is real and $R_{n,-l} = R_{nl}$.)

The function $R_{nl}(\rho)$ of Eq. (37) is real valued, and since the image intensity function $f(x,y)$ is also real, it is often convenient to work with real expansions and real-valued Zernike moments. The real expansion corresponding to Eq. (39) is

$$f(x,y) = \sum_n \sum_l (C_{nl}\cos l\theta + S_{nl}\sin l\theta) R_{nl}(\rho), \tag{42}$$

where l now takes on only positive integral values subject to Eq. (40).

The real Zernike moments are

$$\begin{bmatrix} C_{nl} \\ S_{nl} \end{bmatrix} = [(2n+2)/\pi] \iint dx\,dy f(x,y) R_{nl}(\rho) \begin{bmatrix} \cos l\theta \\ \sin l\theta \end{bmatrix}, \quad (43)$$

for l not zero and

$$C_{n0} = A_{n0} = (1/\pi) \iint dx\,dy f(x,y) R_{n0}(\rho), \quad (44)$$

while

$$S_{n0} = 0.$$

[In the diffraction theory of aberrations, only the cosine terms in Eq. (42) occur for axially symmetric systems. We have in the present paper need of the general case.]

The connection between real and complex Zernike moments is ($l > 0$)

$$\begin{aligned} C_{nl} &= 2\,\mathrm{Re}(A_{nl}), \\ S_{nl} &= -2\,\mathrm{Im}(A_{nl}), \\ A_{nl} &= (C_{nl} - iS_{nl})/2 = (A_{n,-l})^*. \end{aligned} \quad (45)$$

D. Relation between Zernike and the usual moments

The Zernike moments are related to the usual moments μ_{pq}. Thus once μ_{pq} have been calculated by integration (and normalized), we have the Zernike moments also, although in practical applications it is much simpler to calculate the Zernike moments directly from their definition Eq. (41).

The radial polynomials have the form

$$R_{nl}(\rho) = \sum_{k=l}^{n} B_{nlk} \rho^k, \quad (46)$$

where n-k is even and the coefficients $\{B_{nlk}\}$ are given in Ref. 15. Using Eq. (46) and Eq. (41), one gets

$$A_{nl} = [(n+1)/\pi] \sum_{k=l}^{n} \sum_{j=0}^{q} \sum_{m=0}^{l} (-i)^m \binom{q}{j} \binom{l}{m} B_{nlk} \times \mu_{k-2j-l+m,\,2j+l-m}, \quad (47)$$

where $q = (k-l)/2$. For reference purposes we quote the following cases of the last equation:

$$\begin{aligned} A_{00} &= \mu_{00}/\pi = 1/\pi, \\ A_{11} &= A_{1,-1} = 0, \\ A_{22} &= 3(\mu_{02} - \mu_{20} - 2i\mu_{11})/\pi, \\ A_{20} &= 3(2\mu_{20} + 2\mu_{02} - 1)/\pi, \\ A_{33} &= 4[\mu_{03} - 3\mu_{21} + i(\mu_{30} - 3\mu_{12})]/\pi, \\ A_{31} &= 12[\mu_{03} + \mu_{21} - i(\mu_{30} + \mu_{12})]/\pi, \\ A_{44} &= 5[\mu_{40} - 6\mu_{22} + \mu_{04} + 4i(\mu_{31} - \mu_{13})]/\pi, \\ A_{42} &= 5\{4(\mu_{04} - \mu_{40}) + 3(\mu_{20} - \mu_{02}) \\ &\quad -2i[4(\mu_{31} + \mu_{13}) - 3\mu_{11}]\}/\pi, \\ A_{40} &= 5[6(\mu_{40} + 2\mu_{22} + \mu_{04}) - 6(\mu_{20} + \mu_{02}) + 1]/\pi. \end{aligned} \quad (48)$$

E. Behavior under rotation

Consider a rotation of the image through the angle θ_0. In the passive viewpoint of symmetry operations, this would correspond to transforming to new coordinates:

$$\begin{aligned} x' &= x\cos\theta_0 - y\sin\theta_0, \\ y' &= x\sin\theta_0 + y\cos\theta_0. \end{aligned} \quad (49)$$

Instead of this viewpoint we use only one set of image plane coordinates and rotate instead the image: the original image irradiance function $f(\rho,\theta)$ becomes after rotation

$$f'(\rho,\theta) = f(\rho,\theta - \theta_0), \quad (50)$$

and the new Zernike moment is

$$(A_{nl})' = [(n+1)/\pi] \iint \rho\,d\rho\,d\theta f(\rho,\theta-\theta_0) \times R_{nl}(\rho) \exp(-il\theta),$$

which after manipulation becomes

$$(A_{nl})' = A_{nl} \exp(-il\theta_0). \quad (51)$$

Thus the Zernike moments have simple rotational transformation properties; each (complex) Zernike moment merely acquires a phase factor on rotation. From Eq. (51) and Eq. (45), it is straightforward to find that the real-valued Zernike moments transform as

$$\begin{aligned} (C_{nl})' &= C_{nl}\cos l\theta_0 - S_{nl}\sin l\theta_0, \\ (S_{nl})' &= C_{nl}\sin l\theta_0 + S_{nl}\cos l\theta_0. \end{aligned} \quad (52)$$

[The simplicity of the Zernike moments's transformation property [Eq. (51) and Eq. (52)] under image rotation should be contrasted with the behavior of the usual moments as shown in Eq. (36).]

F. Behavior under reflection

A true invariant (scalar) is unchanged by a reflection while a pseudoinvariant (pseudoscalar) changes sign. This means an object and its mirror image will produce the same true invariant, but they may be distinguished if one looks at pseudoinvariants.

Consider the general case of reflection across a line through the origin, rotated through positive angle θ_0 with respect to the y axis. The image point (x,y) then becomes the image point (x',y') where

$$\begin{aligned} x' &= -x\cos 2\theta_0 - y\sin 2\theta_0, \\ y' &= -x\sin 2\theta_0 + y\cos 2\theta_0. \end{aligned} \quad (53)$$

Note that this transformation P is self-inversive, $P^2 = 1$, and has determinant $= -1$. The fact that this transformation depends on $2\theta_0$ is a consequence of the reflection line having no unique direction: it is unchanged by 180° rotation.

The image intensity function $f(x,y)$ is changed by the reflection to

$$f'(x,y) = f(x',y'), \quad (54)$$

and corresponding to Eq. (27) we have

$$\begin{aligned} \rho' &= \rho, \\ \theta' &= 2\theta_0 - \theta. \end{aligned} \quad (55)$$

The new Zernike moment is

$$(A_{nl})' = [(n+1)/\pi] \iint dx\,dy f(x,y)\, R_{nl}(\rho) \times \exp[-il(2\theta_0 - \theta)]$$

or

$$(A_{nl})' = (A_{nl})^* \exp(-i2l\theta_0), \quad (56)$$

and corresponding to Eq. (53) the real Zernike moments transform as

$$\begin{aligned} (C_{nl})' &= C_{nl}\cos 2l\theta_0 + S_{nl}\sin 2l\theta_0, \\ (S_{nl})' &= +C_{nl}\sin 2l\theta_0 - S_{nl}\cos 2l\theta_0. \end{aligned} \quad (57)$$

G. Construction of invariants and pseudoinvariants

Combinations of image moments may be determined that are independent of the object's size, lateral displacement, and orientation. The first two properties have already been taken care of by the use of normalized, central moments. We now construct quantities invariant under rotation and reflection.

We work with complex Zernike moments

$$A_{nl} = |A_{nl}| \exp(i\phi_{nl}), \tag{58}$$

and the basic results being applied are the rotation behavior [Eq. (51)] and the reflection behavior [Eq. (56)] of the Zernike moments. (We also wish to make sure that the invariants we construct are real valued.)

The first two true invariants are A_{00} and $A_{11}\,A_{1,-1} = |A_{11}|^2$, but these are trivial [same values for all images; see Eq. (48)] and will not be counted.

In second order we have the two true invariants

$$S_1 = A_{20}, \tag{59}$$

$$S_2 = A_{22}A_{2,-2} = |A_{22}|^2, \tag{60}$$

which are unchanged under any orthogonal transformation, proper or improper.

In third order we have to work with the four moments A_{33}, A_{31}, $A_{3,-1}$, $A_{3,-3}$. The following two true invariants are immediately constructed:

$$S_3 = |A_{33}|^2, \tag{61}$$

$$S_4 = |A_{31}|^2. \tag{62}$$

The maximum possible number of independent third-order invariants is obviously four because, at this point, given the invariants, we could solve for the moments. So we should seek two more third-order invariants. One might think a term such as

$$A_{33}(A_{3,-1})^3 = A_{33}[(A_{31})^*]^3$$

would serve as an additional invariant. It has two shortcomings: While it is rotationally invariant, under an improper transformation, it changes to

$$(A_{33})^*(A_{31})^3.$$

In addition, both of these terms are complex valued. However, a third true, real-valued, scalar is obviously the sum of these two:

$$S_5 = A_{33}[(A_{31})^*]^3 + \text{c.c.} = 2|A_{33}|\,|A_{31}|^3\cos(\phi_{33} - 3\phi_{31}), \tag{63}$$

where c.c. is the complex conjugate of the preceding term. We get the first pseudoscalar by using the difference

$$P_1 = -i\{A_{33}[(A_{31})^*]^3 - \text{c.c.}\} = 2|A_{33}||A_{31}|^3\sin(\phi_{33} - 3\phi_{31}). \tag{64}$$

No further independent invariants exist using only third-order moments. However, by combining third- and second-order invariants we do get another independent invariant:

$$S_6 = (A_{31})^2(A_{22})^* + \text{c.c.} = 2|A_{31}|^2A_{22}\cos(2\phi_{31} - \phi_{22}). \tag{65}$$

[Taking instead a minus sign in the first line of Eq. (65) would give another pseudo-scalar, but we avoid listing further pseudoscalars for now.]

At this point we note the important fact that given S_3 through S_6 we cannot solve for the four third-order moments because ϕ_{22} also appears. There will always occur one too many phase angles to allow one to solve for the moments, given the invariants. This, however, just corresponds to the one degree of rotational freedom of the image plane. That is, while we are constructing valid invariants, we cannot actually invert the invariant defining equations to find the moments until we have specified the target orientation in the image plane, which we can do, for example, by specifying ϕ_{22}. These remarks are crucial for determining whether a set of invariants that one has constructed are functionally independent. For example, instead of S_6, one could have used

$$(A_{33})^2[(A_{22})^*]^3 + \text{c.c.} = 2|A_{33}|^2|A_{22}|^3\cos(2\phi_{33} - 3\phi_{22})$$

as a true invariant, but not (usefully) both this and S_6, as it obviously is already determined by the preceding invariants.

Now consider the fourth-order moments A_{44}, A_{42}, A_{40}, $A_{4,-2}$, $A_{4,-4}$. Again we immediately have the invariants

$$S_7 = |A_{44}|^2, \tag{66}$$

$$S_8 = |A_{42}|^2, \tag{67}$$

$$S_9 = A_{40}. \tag{68}$$

The remaining invariant consisting only of fourth-order moments is

$$S_{10} = (A_{44})^*(A_{42})^2 + \text{c.c.} = 2|A_{44}|\,|A_{42}|^2\cos(\phi_{44} - 2\phi_{42}), \tag{69}$$

and as a fifth independent invariant we can choose

$$S_{11} = A_{42}(A_{22})^* + \text{c.c.} = 2|A_{42}|\,|A_{22}|\cos(\phi_{42} - \phi_{22}). \tag{70}$$

For the fifth-order moments A_{55}, A_{53}, A_{51}, $A_{5,-1}$, $A_{5,-3}$, $A_{5,-5}$, we seek six invariants. We get three easily:

$$S_{12} = |A_{55}|^2, \tag{71}$$

$$S_{13} = |A_{53}|^2, \tag{72}$$

$$S_{14} = |A_{51}|^2. \tag{73}$$

For the first time we can construct three more invariants using only the fifth-order moments (and these we might expect complete our set of six invariants). They are

$$(A_{55})^{*3}(A_{53})^5 + \text{c.c.} = 2|A_{55}|^3|A_{53}|^5\cos(3\phi_{55} - 5\phi_{53}),$$

$$(A_{55})^*(A_{51})^5 + \text{c.c.} = 2|A_{55}||A_{51}|^5\cos(\phi_{55} - 5\phi_{51}),$$

$$(A_{53})^*(A_{51})^3 + \text{c.c.} = 2|A_{53}||A_{51}|^3\cos(\phi_{53} - 3\phi_{51}).$$

These are six true invariants, but any of the last three is functionally dependent on the other five. To see this, we try to invert the six equations to find the six fifth-order moments. We immediately get three moduli from Eq. (71) through Eq. (73), leaving the last three equations to get the three phases. Inverting the cosines, we get equations of the form

$$3\phi_{55} - 5\phi_{53} = a,$$

$$\phi_{55} - 5\phi_{51} = b,$$

$$\phi_{53} - 3\phi_{51} = c,$$

where a, b, c are known quantities. This set has zero determinant showing that one cannot solve for the phases and, hence, the six invariants were functionally dependent. Again, this is just a reflection of the fact that the image orientation has not been specified, and one cannot find the phase of any A_{nl} ($l \neq 0$) until, e.g., ϕ_{22} has been specified.

Note also that it is a feature of this method that while we use nonlinear methods to construct invariants, in order to check for functional dependence of the invariants, one has only to consider a linear algebra problem in the phases as was done above. This is much more tractable than the general mathematical requirement to consider a Jacobian determinant to check functional invertability.

To get the needed three remaining fifth-order invariants, we pick

$$S_{15} = (A_{51})^* A_{31} + \text{c.c.}, \tag{74}$$

$$S_{16} = (A_{53})^* A_{33} + \text{c.c.}, \tag{75}$$

$$S_{17} = (A_{55})^* (A_{31})^5 + \text{c.c.} \tag{76}$$

These choices are made for later convenience. As a general rule, one should build invariants using the lowest possible powers of the Zernike moments. In Appendix A we express the preceding invariants in terms of the usual normalized, central moments μ_{jk}, and the resulting expressions are simpler if we avoid high powers of the Zernike moments.

Finally, it is obvious that wherever we constructed a true, real-valued invariant by taking a quantity plus its complex conjugate, we could have obtained the corresponding, real-valued, pseudoinvariant by taking $-i$ times the quantity minus its complex conjugate.

The reader will now understand how to construct independent sets of Zernike moment invariants to arbitrarily high order and between the text and Appendix B, we have listed results up through the eighth order.

IV. APPLICATIONS OF MOMENT INVARIANTS

In Figs. 4(a)–4(e), we show the Zernike moment invariants for several simple input images. Again, a 21 × 21 pixel image space was used. The numbers plotted are actually statistical averages of the numerically calculated Zernike moment invariants when the input image was rotated through 360° at finite steps. If there were no quantization errors associated with rotating the image and no numerical errors associated with the numerical integrals necessary to obtain the Zernike moments [which were calculated directly from their defining equation (41)], then the Zernike invariants would be truly invariant as the image rotates. The error sources mentioned produce standard deviations of from a few percent to 10 or 20 percent of the associated average values. In all Figs. 4(a)–4(e), we have calculated 43 quantities. The first 41 are the invariants S_1 through S_{41}, which include all Zernike invariants through eighth order. The last two entries, the 42nd and 43rd, are the two pseudoinvariants P_1 and P_2 from Appendix A. While one pseudoinvariant is in principle sufficient to identify a mirror image, it is better to calculate several in case some are fortuitously numerically small and buried in noise.

It is obvious that for this set of calculations, an image is identified as a point in a 41-dimensional space. (The last two quantities which are pseudoscalars serve only to identify whether one has an image or its mirror image and are not functionally independent of the remaining 41 true scalars.) However, for visual comparison purposes, we plot in Figs. 4(a)–4(e) the numerical values of the components of the 41-dimension image vector. There is no significance to the connecting lines, the Zernike invariants exist only at integer values.

The first invariant S_1 measures the normalized size of the image, i.e., the radius of gyration of the irradiance distribution when the total image power is normalized to unity. The second moment S_2 measures the skinniness of the distribution. It is zero for a circle or a square. These two invariants alone were used by Hu[5] for alphabetical character recognition schemes, while Dudani *et al.*[6] also included S_3–S_6 in aircraft recognition schemes. (Actually, they used equivalent moment invariants not based on Zernike moments.) The number of such invariants that must be used for pattern recognition purposes obviously depends on the complexity of the class of recognition images. For example, the first two invariants may suffice to recognize alphabetical characters. However, the results of Sec. II indicate that if one wishes to reconstruct from their moments images of the same general complexity as alphabetical characters, then even including eighth-order moments is not expected to be sufficient.

We now point out that the Zernike moment invariants furnish an optimal means to code the essential features of an image pattern, i.e., they contain information about the image that is independent of the image size, centroid position, and relative angular orientation. The missing features, if needed, are supplied by the second- and lower-order moments. Therefore, given the Zernike invariants, one can solve for the Zernike moments and, using the techniques of Sec. II, reconstruct the image to a given order of accuracy. If only Zernike invariants are used (and not the information in second- and lower-order moments), then one will get a normalized reconstruction, i.e., one with standard size and one which is centered and unrotated.

The moment invariants furnish a natural method for the recognition of two-dimensional patterns and at this point the recognition problem becomes a statistical one; for example, how should one define a weighted metric in an n-dimensional recognition space—a difficult problem discussed in Ref. 6. At present, if moment methods are used for three-dimensional object recognition, one must consider different views of a given object as different two-dimensional patterns to be recognized. Thus the recognition space is enlarged to contain information about all the relevant Euler angles of the set of recognition objects.

As mentioned earlier, image moments may be calculated with a coherent optical processor by using the Fourier transforming properties of a converging lens.[16] Moments are then determined as partial derivatives of the image Fourier transform evaluated at the origin of Fourier space. The difficulty here is that one cannot simply place a detector array in the Fourier plane since both the real and imaginary parts of the Fourier transform must be measured and not just its modulus. The details of an optical arrangement to perform the necessary calculation are being reported elsewhere.[17]

An alternative approach to calculating irradiance moments

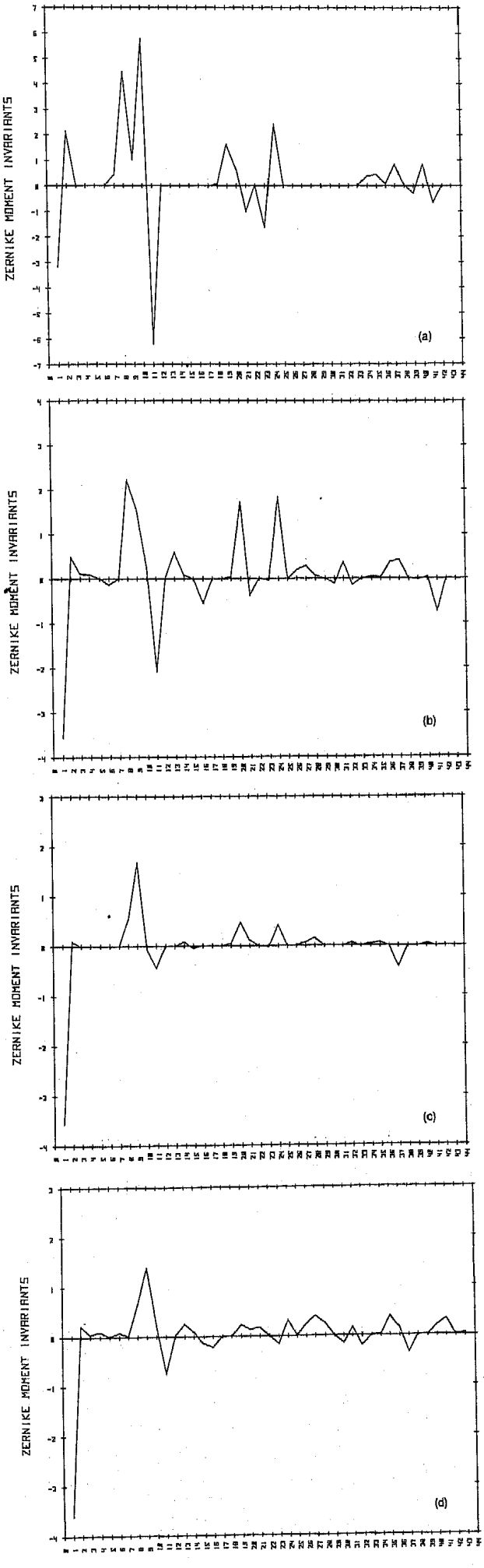

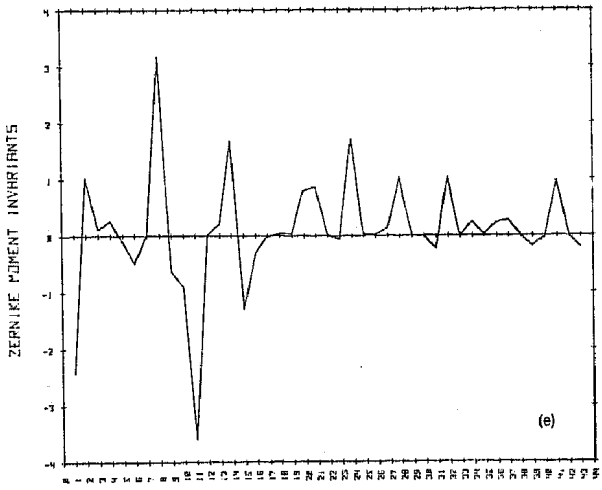

FIG. 4. Zernike moments invariants for: (a) a centered, constant irradiance, rectangle of 5 by 19 pixels; (b) a centered 5 by 13 pixel rectangle with a small 3 by 3 pixel square sitting on the left-hand end of the big rectangle; (c) the letter E (same as Fig. 2); (d) the letter F (same as Fig. 3); (e) the letter C. For these figures the Zernike polynomials were normalized to unity inside the unit circle rather than using the norm of Eq. (38).

using optical processing techniques has recently been described by Casasent and Psaltis.[18]

ACKNOWLEDGMENT

The author expresses his appreciation to Lawrence Sher, Paul Merritt, and Carey O'Bryan for their support, suggestions, and critical comments regarding this paper.

APPENDIX A: ZERNIKE MOMENT INVARIANTS EXPRESSED IN TERMS OF USUAL MOMENTS

Second Order

$$S_1 = A_{20} = 3[2(\mu_{20} + \mu_{02}) - 1]/\pi,$$
$$S_2 = |A_{22}|^2 = 9[(\mu_{20} - \mu_{02})^2 + 4(\mu_{11})^2]/\pi^2.$$

Third Order

$$S_3 = |A_{33}|^2 = 16[(\mu_{03} - 3\mu_{21})^2 + (\mu_{30} - 3\mu_{12})^2]/\pi^2,$$
$$S_4 = |A_{31}|^2 = 144[(\mu_{03} + \mu_{21})^2 + (\mu_{30} + \mu_{12})^2]/\pi^2,$$
$$S_5 = (A_{33})^* (A_{31})^3 + \text{c.c.}$$
$$= \frac{13\,824}{\pi^4}\{(\mu_{03} - 3\mu_{21})(\mu_{03} + \mu_{21}) \times [(\mu_{03} + \mu_{21})^2 - 3(\mu_{30} + \mu_{12})^2] - (\mu_{30} - 3\mu_{12})(\mu_{30} + \mu_{12}) \times [(\mu_{30} + \mu_{12})^2 - 3(\mu_{03} + \mu_{21})^2]\},$$
$$S_6 = (A_{31})^2 A_{22}^* + \text{c.c.}$$
$$= \frac{864}{\pi^3}\{(\mu_{02} - \mu_{20})[(\mu_{03} + \mu_{21})^2 - (\mu_{30} + \mu_{12})^2] + 4\mu_{11}(\mu_{03} + \mu_{21})(\mu_{30} + \mu_{12})\}.$$

Fourth Order

$$S_7 = |A_{44}|^2 = 25[(\mu_{40} - 6\mu_{22} + \mu_{04})^2 + 16(\mu_{31} - \mu_{13})^2]/\pi^2,$$
$$S_8 = |A_{42}|^2 = 25\{[4(\mu_{04} - \mu_{40}) + 3(\mu_{20} - \mu_{02})]^2 + 4[4(\mu_{31} + \mu_{13}) - 3\mu_{11}]^2\}/\pi^2,$$

$$S_9 = A_{40}$$
$$= 5[6(\mu_{40} + 2\mu_{22} + \mu_{04}) - 6(\mu_{20} + \mu_{02}) + 1]/\pi,$$

$$S_{10} = (A_{44})^*(A_{42})^2 + \text{c.c.} = \frac{250}{\pi^3}((\mu_{40} - 6\mu_{22} + \mu_{04})$$
$$\times \{4(\mu_{04} - \mu_{40}) + 3(\mu_{20} - \mu_{02})]^2 - 4[4(\mu_{31} + \mu_{13}) - 3\mu_{11}]^2\}$$
$$- 16[4(\mu_{04} - \mu_{40}) + 3(\mu_{20} - \mu_{02})]$$
$$\times [4(\mu_{31} + \mu_{13}) - 3\mu_{11}](\mu_{31} - \mu_{13})),$$

$$S_{11} = A_{42}(A_{22})^* + \text{c.c.}$$
$$= \frac{30}{\pi^2}\{[4(\mu_{04} - \mu_{40}) + 3(\mu_{20} - \mu_{02})](\mu_{02} - \mu_{20})$$
$$+ 4\mu_{11}[4(\mu_{31} + \mu_{13}) - 3\mu_{11}]\}.$$

The following are pseudo-invariants:

$$P_1 = -i(A_{33}^* A_{31}^3 - \text{c.c.})$$
$$= 13\,824\{(\mu_{30} - 3\mu_{12})(\mu_{03} + \mu_{21})[(\mu_{03} + \mu_{21})^2$$
$$-3(\mu_{30} + \mu_{12})^2] - (\mu_{03} - 3\mu_{21})(\mu_{30} + \mu_{12})$$
$$\times [(\mu_{30} + \mu_{12})^2 - 3(\mu_{03} + \mu_{21})^2]\}/\pi^4,$$

$$P_2 = -i[(A_{31})^2 (A_{22})^* - \text{c.c.}]$$
$$= 1728\{\mu_{11}[(\mu_{03} + \mu_{21})^2 - (\mu_{30} + \mu_{12})^2]$$
$$- (\mu_{03} + \mu_{21})(\mu_{30} + \mu_{12})(\mu_{02} - \mu_{20})\}/\pi^3.$$

APPENDIX B: HIGHER-ORDER ZERNIKE MOMENT INVARIANTS

For reference purposes we list further independent moment invariants. Between this appendix and the preceding text, results are given for all cases of the Zernike polynomial tables of Ref. 15.

Sixth Order

$$S_{18} = |A_{66}|^2,$$
$$S_{19} = |A_{64}|^2,$$
$$S_{20} = |A_{62}|^2,$$
$$S_{21} = A_{60},$$
$$S_{22} = (A_{66})^*(A_{33})^2 + \text{c.c.},$$
$$S_{23} = (A_{64})^* A_{44} + \text{c.c.},$$
$$S_{24} = (A_{62})^* A_{22} + \text{c.c.}$$

Seventh Order

$$S_{25} = |A_{77}|^2,$$
$$S_{26} = |A_{75}|^2,$$
$$S_{27} = |A_{73}|^2,$$
$$S_{28} = |A_{71}|^2,$$
$$S_{29} = (A_{77})^*(A_{31})^7 + \text{c.c.},$$
$$S_{30} = (A_{75})^* A_{55} + \text{c.c.},$$
$$S_{31} = (A_{73})^* A_{33} + \text{c.c.},$$
$$S_{32} = (A_{71})^* A_{31} + \text{c.c.}$$

Eighth Order

$$S_{33} = |A_{88}|^2,$$
$$S_{34} = |A_{86}|^2,$$
$$S_{35} = |A_{84}|^2,$$
$$S_{36} = |A_{82}|^2,$$
$$S_{37} = A_{80},$$
$$S_{38} = (A_{88})^*(A_{44})^2 + \text{c.c.},$$
$$S_{39} = (A_{86})^* A_{66} + \text{c.c.},$$
$$S_{40} = (A_{84})^* A_{44} + \text{c.c.},$$
$$S_{41} = (A_{82})^* A_{22} + \text{c.c.}$$

* Portions of this paper were presented at the 1979 Annual Meeting of the Optical Society of America.

† Present Address: The Charles Stark Draper Laboratory, Inc., Mail Station 84 555 Technology Square, Cambridge, Mass. 02139.

[1]R. A. Gonsalves, "Phase retrieval from modulus data," J. Opt. Soc. Am. 66, 961–964 (1976).
[2]W. H. Southwell, "Wave-front analyzer using maximum likelihood algorithm," J. Opt. Soc. Am. 67, 396–399 (1977).
[3]S. R. Robinson, "On the problem of phase from intensity measurements," J. Opt. Soc. Am. 68, 87–92 (1978).
[4]A. J. Devaney and R. Childlaw, "On the uniqueness question in the problem of phase retrieval from intensity measurements," J. Opt. Soc. Am. 68, 1352–1354 (1978).
[5]M. K. Hu, "Visual pattern recognition by moment invariants," IRE Trans. Inf. Theory IT-8, 179–187 (1962).
[6]S. A. Dudani, K. J. Breeding, and R. B. McGhee, "Aircraft identification by moment invariants," IEEE Trans. Comput. C-26, 39–45 (1977).
[7]R. O. Duda and P. E. Hart, *Pattern Classification and Scene Analysis* (Wiley, New York, 1973).
[8]N. Bareket and W. L. Wolfe, "Image chopping techniques for fast measurements of irradiance distribution parameters," Appl. Opt. 18, 389–392 (1979).
[9]M. R. Teague, "Automatic image analysis via the method of moments," Laser Digest, Summer 1979, p. 25–43, AFWL, Kirtland AFB, New Mexico (unpublished).
[10]See, for example, N. I. Akhiezer, *The Classical Moment Problem and Some Related Question in Analysis* (Hafner, New York, 1965).
[11]A. Papoulis, *Probability, Random Variables, and Stochastic Processes* (McGraw-Hill, New York, 1965).
[12]A. Sommerfeld, *Partial Differential Equations in Physics* (Academic, New York, 1949).
[13]A. D. Myskis, *Advanced Mathematics for Engineers* (MIR, Moscow, 1975).
[14]R. Courant and D. Hilbert, *Methods of Mathematical Physics, Vol. I* (Interscience, New York, 1953).
[15]M. Born and E. Wolf, *Principles of Optics* (Pergamon, New York, 1975).
[16]J. W. Goodman, *Introduction to Fourier Optics* (McGraw-Hill, San Francisco, 1968).
[17]M. R. Teague, "Optical calculation of image moments," Appl. Opt. 19, 1353–1356, (1980).
[18]D. Casasent and D. Psaltis, "Optical pattern recognition using normalized invariant moments," SPIE Proc. (to be published).

Das Original lässt leider keine bessere Qualität der Reproduktion zu !

Mit freundlichem Gruß
TIB/UB Hannover

Due to bad print quality of the publication, it's not possible to provide you with better duplication!

Best regards
TIB/UB Hannover